# CFD Simulation of flow through pipe fittings

**Prepared by**

**Mukund S**
**BMS College of Engineering, Banglore**

Under the supervision of

**Prof. Manaswita Bose**

**INDIAN INSTITUTE OF TECHNOLOGY BOMBAY**

# ACKNOWLEDGEMENT

The following report was created as a part of FOSSEE semester long internship and I would like to thank FOSSEE, Indian Institute of Technology, Bombay for giving me this opportunity.

I would like to thank my project guide Prof. Manaswita Bose, Mentors Mr. Divyesh Variya and Mr. Ashley Melvin for the support in carrying out simulations through out the internship. I would also like to thank project manager Ms. Swetha Manian for giving me this opportunity.

I would like to extend my gratitude to Head, Department of Energy Science and Engineering, Indian Institute of Technology Bombay for giving the permission to use experimental data for validation and Swapnil Raut for helping with details and support.

**Mukund S**
**BMS College of Engineering, Banglore**
**Date:** September 1, 2021

# Contents

# List of Figures

# List of Tables

# Part I

# Case Study 1: Coefficient of Discharge of an Orifice Meter

# Chapter 1

# Introduction

## 1.1 Aim

The aim of this case study was to determine the Coefficient of discharge of an orifice meter through CFD method. OpenFOAM version 1912 was used for carrying out the simulation. Further, the velocity and pressure contours of the flow were studied and the position of the vena contracta was characterized. The study was performed for a 2-D incompressible flow with water as the working fluid, simpleFoam steady state solver was used and $\kappa$-$\epsilon$ RANS model was adopted to simulate the turbulent flow. The results were viewed in ParaView 5.7.0

## 1.2 Theory

An orifice meter is essentially a cylindrical tube that contains a plate with a thin hole in the middle of it. The thin hole essentially forces the fluid to flow faster through the hole in order to maintain flow rate. The point of maximum convergence (vena contracta) usually occurs slightly downstream from the actual physical orifice. This is the reason why orifice meters are less accurate than venturi meters, as we cannot use the exact location and diameter of the point of maximum convergence in calculations. Beyond the vena contracta point, the fluid expands again and velocity decreases as pressure increases. Figure 1.1 shows an orifice meter with the variable position of vena contracta with respect to the orifice plate. By employing the continuity equation and Bernoullis principle, the volumetric flow
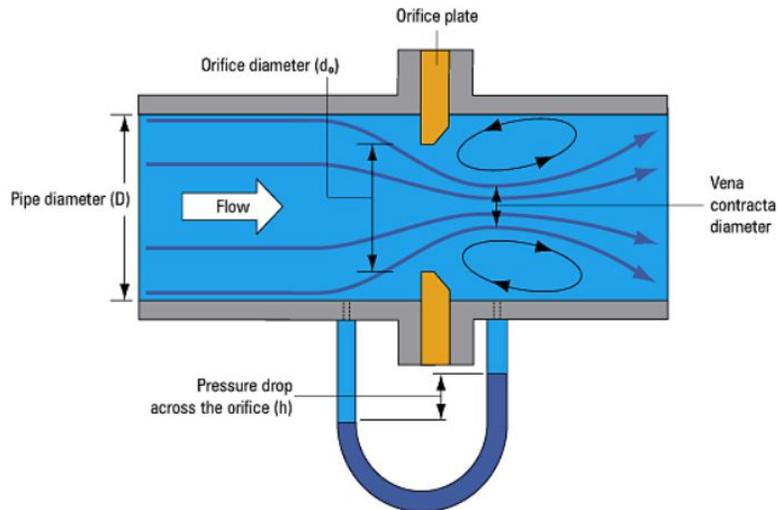
Figure 1.1: Orifice meter ?
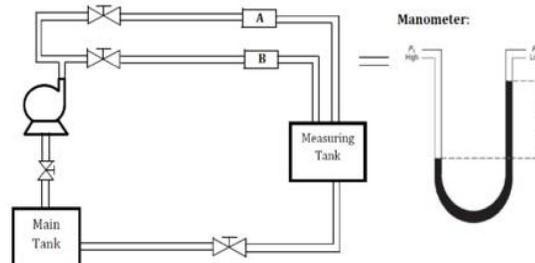
Figure 1.2: Schematic Diagram for Orifice meter B: Orifice meter ?

rate through the orifice meter can be calculated giving the below equation,

$$Q = V_2 S_2 = \frac{C_O S_2 \sqrt{2g\delta H}}{\sqrt{1 - \beta^4}} \tag{1.1}$$

where $C_O$ is the orifice discharge coefficient, $S_2$ is the area of cross-section of the orifice, $V_2$ is the flow velocity through the orifice, $\beta$ is the ratio of the orifice diameter to that of the pipe, $\delta H$ is the manometric height difference Œ (specific gravity of manometric fluid specific gravity of water), and g is the acceleration due to gravity. Figure 1.2 depicts the schematic layout of the test setup consisting of the orifice meter ? ?.

## 1.3 Problem Statement

The primary objective of the case study is to simulate turbulent flow inside an orifice meter and later calculate the coefficient of discharge using the CFD result and compare it with the experimental results. The dimensions of the orifice geometry are considered from the lab manual. The simulations were conducted for 15 different cases with reynolds number varying from the range of 6000 to 20000. To study this turbulent flow, simpleFoam solver is used.

## 1.4 Schematic Diagram

The dimensions of the geometry is given below

Length of the orifice meter = 13mm

Entrance diameter, D1 = 16mm

Diameter of the orifice, D2= 8mm

Cross-sectional area of the orifice, $S_2 = \frac{\pi(D_2)^2}{4} = 5.026 \times 10^{-5}$

$\beta = \frac{D_2}{D_1} = 0.5$

The geometry of the orifice meter is shown in the Figure 1.3.



Figure 1.3: Axisymmetric Geometry of orifice meter

# Chapter 2

# OpenFOAM base case

## 2.1  pitzDaily

The base case considered for the simulation of the orifice meter is the pitzDaily case. This case can be found under the incomressible section, simpleFoam subsection. The directory for this is
\\*OpenFOAM-v1912*\\*tutorials*\\*incompressible*\\*simpleFoam*\\*pitzDaily*.
Based on the experimental work of Pitz and Daily (1981). It features a backward facing step. Such a "classic" case is instructive for comparing different turbulence models with respect to the size and shape of the recirculation zone[internet reference]. pitzDaily introduces the dollowing concepts for the first time:

- Mesh creation using blockMesh and also mesh grading capability

- Turbulent steady flow.

## 2.1.1  Folder Structure

Any case file in OpenFOAM has three folders, called the 0, constant and the system. The constant contains coefficient values that will be used in equations and also things which will remain constant like the mesh, material properties, environmental constants which the solver uses, the 0 folder contains the initial and boundary conditions, and the system folder contains the configuration files for the mesh and also how the solver will be executed, schemes and methods to use and controls for the simulation.

Table 2.1: Folder contents

| Directories | Constant | 0 | System |
|---|---|---|---|
| Sub-directories | transportProperties turbulenceProperties polyMesh | U p nut epsilon k | blockMeshDict fvSchemes fvSolution |

## 2.2 Solver

OpenFOAM or Open-source Field Operation And Manipulation is an open-source C++ tool used for solving continuum mechanics problems, with a focus on Finite Volume Method (FVM). The software package includes solver codes for different kinds of transport phenomena, varying from simple laplacian solver called laplacianFoam to complex multiphase flow, compressible flow, heat transfer, incompressible flow, and many more. The flagship solver and most commonly used solver is simpleFoam. simpleFoam is a steady-state solver for incompressible, turbulent flow. It utilizes the SIMPLE (Semi-Implicit Method for Pressure Linked Equations) algorithm. It is an approximation of the velocity field which is obtained by solving the momentum equation. The pressure gradient term is calculated using the pressure distribution from the previous iteration or an initial guess. The pressure equation is formulated and solved to obtain the new pressure distribution. Velocities are corrected and a new set of conservative fluxes is calculated. The solver used for this case study is simpleFoam, it employs SIMPLE algorithm. The case study considered is a steady state, incompressible, three-dimensional flow. The set of Navier Stokes equations governing the flow is given below.

The continuity equation is given as,

$$\nabla . \vec{u} = 0 \tag{2.1}$$

The momentum equation is given as.

$$\frac{\partial \vec{u}}{\partial t} + \nabla . [\vec{u}\vec{u}] = -\frac{1}{\rho}\nabla p + \nu \nabla^2 \vec{u} \tag{2.2}$$

Where, $\vec{u}$ is velocity, p-pressure; $\nu$ is kinematic viscosity The discretized momentum equation and pressure correction equation are solved implicitly, where the

velocity correction is solved explicitly. This is the reason why it is called "Semi-Implicit Method".

## 2.2.1   Turbulence Model

The turbulence model considered for the simulation is $\kappa$ -$\epsilon$ RANS model. $\kappa$ -$\epsilon$ model solves two additional equations, for turbulent kinematic energy $\kappa$ and rate of dissipation of turbulence energy $\epsilon$ It performs poorly for complex flows involving severe pressure gradient, separation, strong streamline curvature. Suitable for initial iterations, initial screening of alternative designs, and parametric studies. Can be only used with wall functions. The equations for the $\kappa$ -$\epsilon$ RANS model is below,

$$\frac{\partial(p\kappa)}{\partial t} + \frac{\partial(p\kappa u_i)}{\partial x_i} = \frac{\partial}{\partial x_j}[\frac{\mu_t}{\sigma_\kappa}\frac{\partial\kappa}{\partial x_j}] + 2\mu_t E_{ij}E_{ij} - \rho\epsilon \tag{2.3}$$

$$\frac{\partial(p\epsilon)}{\partial t} + \frac{\partial(p\epsilon u_i)}{\partial x_i} = \frac{\partial}{\partial x_j}[\frac{\mu_t}{\sigma_\kappa}\frac{\partial\kappa}{\partial x_j}] + C_{1\epsilon}\frac{\epsilon}{\kappa}2\mu_t E_{ij}E_{ij} - C_{2\epsilon}\rho\frac{\epsilon^2}{\kappa} \tag{2.4}$$

where $u_i$ represents velocity component in corresponding direction, $E_{ij}$ represents component of rate of deformation, and $\mu_t$ represents eddy viscosity. The default value of model coefficients **?**: $C_{1\epsilon}$, $C_{2\epsilon}$, $\sigma_\kappa$, $\sigma_\epsilon$ and $C\mu$ have been used.

# Chapter 3

# OpenFOAM Case Modifications

Using the pitzDaily case, modifications were made with the geometry, the mesh used, boundary conditions applied to it, and the control parameters which are going to be explained further in the below sections.

## 3.1 Pre-processing

The model was created using the dimensions from the manual provided. To simplify the calculation an axisymmetric wedge was created. In OpenFOAM to make the axisymmetric wedge the angle should be 5 degrees. The upstream length and downstream length was taken to be 320mm and axis along Z direction.

The mesh and geometry was created using the blockMesh utility. The blockMeshDict file from the base case was modified to create the axisymmetric model of the orifice geometry. convertToMeters, the very first line of blockMeshDict file is changed, by default the units used in OpenFOAM are in meters. Since the geometry is in millimetres a conversion factor from meters to millimetres was used, replacing 0.01 to 0.001.

The co-ordinates of the geometry are entered in the vertices column of the file. It is entered as x, y, and z coordinate values. X represents the radial distance; Y represents the angular axis and Z represents the axial length of the geometry. Therefore the coordinate axis can be obtained by simple trigonometric formula of $tan = \frac{Oppositeside}{adjacentside}$. The geometry is divided into blocks for Meshing purposes. There are totally 5 blocks. It was made using hexahedral blocks with simplegrading 1 in all directions. In the axisymmetric geometry, the front, back panels, and the axis are additional boundaries. Proper patchfields are assigned to them, for

the front and back panels, boundary patch assigned is wedge and for the axis it is given as empty. Using the blockMesh utility, the mesh was generated and with checkMesh, the quality of the mesh was determined.

## 3.2   Boundary conditions

The initial and boundary conditions are included in the 0 folder as k, epsilon, nut,p, and U. The boundary conditions are summarised in the Table 3.1. In all the files

Table 3.1: Boundary conditions

|         | inlet | outlet | wall |
|---------|-------|--------|------|
| epsilon | turbulentMixingLengthDissipationRateInlet | zeroGradient | epsilonWallFunction |
| k | turbulentIntensityKineticEnergyInlet | zeroGradient | kqRWallFunction |
| nut | calculated | calculated | nutkWallFunction |
| p | zeroGradient | fixedValue | zeroGradient |
| U | flowRateInletVelocity | zeroGradient | noSlip |

in 0 folder, the axis, front_back_pos and front_back_neg were given the boundary condition of empty, wedge and wedge respectively. The value for $\kappa$ and $\epsilon$ were determined using the below equations

$$\kappa = \frac{3}{2}(uI)^2 \tag{3.1}$$

$$\epsilon = \frac{C_\mu \kappa^{1.5}}{0.07l} \tag{3.2}$$

where u is the free stream velocity, I is the turbulence intensity, $C_\mu$ is the model coefficient, l is the characteristic length.

## 3.3   Physical properties

The working fluid for the simulation is water. The density considered is 1000 kg/ $m^3$, with a kinematic viscosity of $1 \times 10^{-06}$ $m^2/s$. So the value in the transport-Properties file was changed to $1 \times 10^{-06}$ from $1 \times 10^{-05}$ and the transportModel remained as it is to Newtonian.

## 3.4 fvSchemes & fvSolution

fvSchems and fvSolutions are found under the constant folder. fvSolution directory contains equation solvers, algorithms and tolerances. No changes were done to this file, the tolerances for the residuals were pre-set to a value of 1e-05 and it was not changed. The numerical schemes for the simulation are entered in the fvSchemes dictionary. No changes were made in this file directory.

## 3.5 Control parameters

The OpenFOAM solvers begin all runs by setting up a database. The database controls I/O and, since output of data is usually requested at intervals of time during the run, time is an inextricable part of the database. The controlDict dictionary sets input parameters essential for the creation of the database. Here the endTime was changed to 10000, i.e., maximum iterations were 10000. startTime was 0 and writeInterval was set to every 100 iterations with 1 as deltaT as it was a steady state analysis.

## 3.6 Post-processing

After the simulation has been completed, the results were viewed in ParaView. To do this, first the results obtained were converted into viewable file using the command *touch suitable_file_name.foam*. A file with .foam extension was created. In this file, the results was viewed, the various contours of the solution was visualised, streamlines were plotted and the data were analysed with the in-built plotting options available.

# Chapter 4

# Results

Steady state simulations were performed using SIMPLE algorithm for $\kappa$ -$\epsilon$ RANS model. The obtained CFD results have been compared with the experimental results for the coefficient of discharge. Post-processing was done using paraview.

## 4.1   Numerical Results

The post-processing of the simulation was done in ParaView for all the 15 simulations. The pressure and velocity contours of the simulation is shown below.
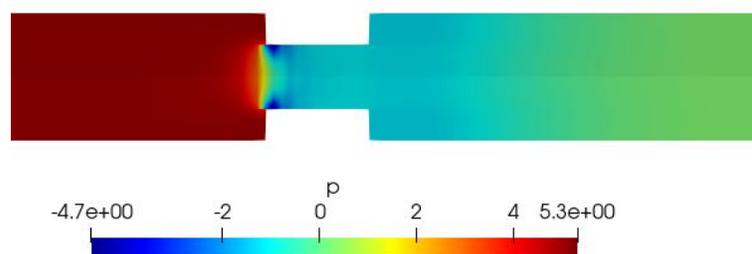


Figure 4.1: Pressure contour

As we can see form the Figure 4.1 and Figure 4.2, as the water flows from a narrowing orifice plate, the flow forms a free flowing jet in the downstream fluid. The velocity is at its maximum. The separation of boundary layer is seen at the downstream side of orifice plate. The turbulent and wake region, together with re-circulation zones can be seen just downstream of orifice meter**?**. Figure 4.3- Figure 4.6 show pressure and velocity contours for two different Reynolds number
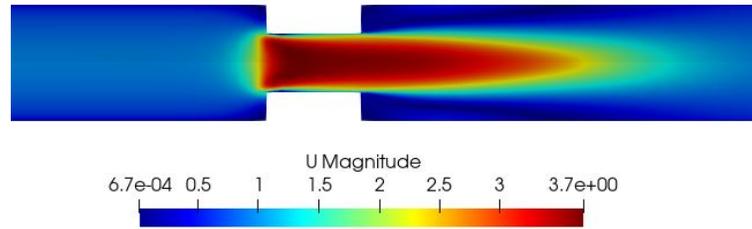
Figure 4.2: Velocity contour

regime. Figure 4.3 and 4.4 are for Reynolds number of 15090, and Figure 4.5 and 4.6 are for Reynolds number of 10650.
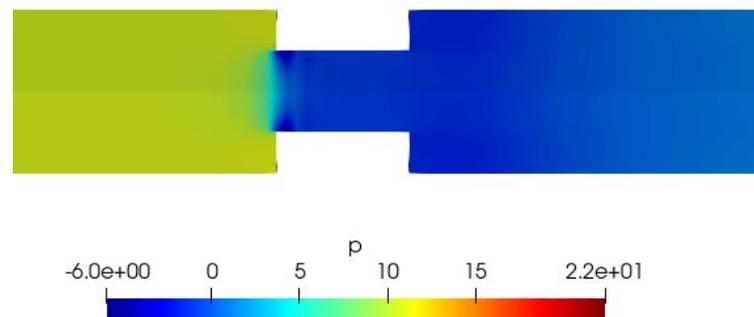
Figure 4.3: Pressure contour for higher Reynolds number

Figure 4.7 shows the developed velocity profile upstream of orifice just before the entrance. Due to the no-slip condition, there is velocity gradient near the walls. This region is often very thin, and it is then called a boundary layer **?**. This graph tells us the velocity is developed and adequate length is given the downstream for the pressure recovery. The evolution of the solution for pressure and velocity is shown above. The pressure was plotted along the axis length as shown in Figure 4.8. The pressure just before the orifice is high and after the orifice there is drop in the pressure. This corresponds to the pressure contour in the Figure 4.1. Figure 4.9 shows the velocity along the axial length of the orifice meter. The velocity remains constant until the mouth of the orifice and then there is a sudden increase as the
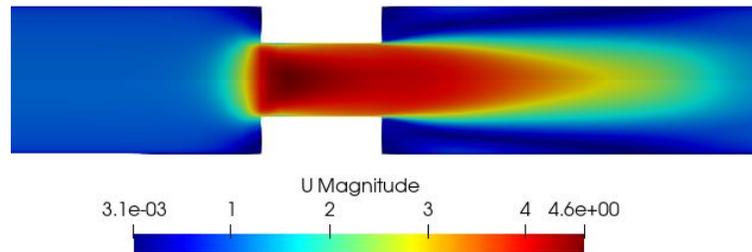
Figure 4.4: Velocity contour for higher Reynolds number
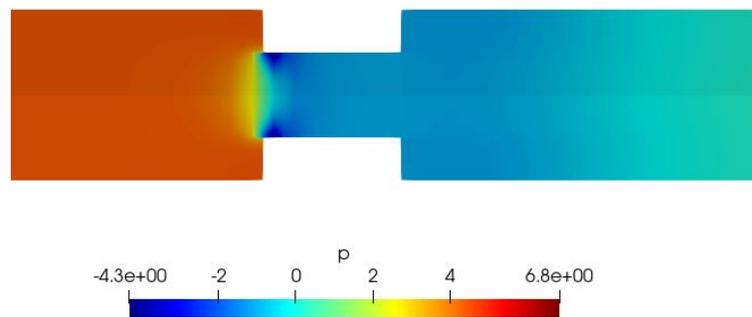


Figure 4.5: Pressure contour for lower Reynolds number
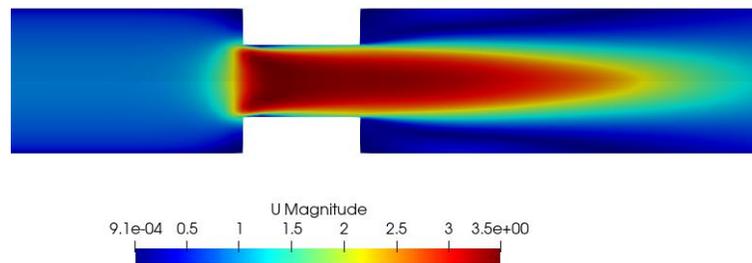


Figure 4.6: Velocity contour for lower Reynolds number

fluid enters the orifice plate. The maximum region of the velocity is called as the vena-contracta and can be seen in velocity contour, Figure 4.2. The streamlines for

fossee
b e t t e r
e d u c a t i o n
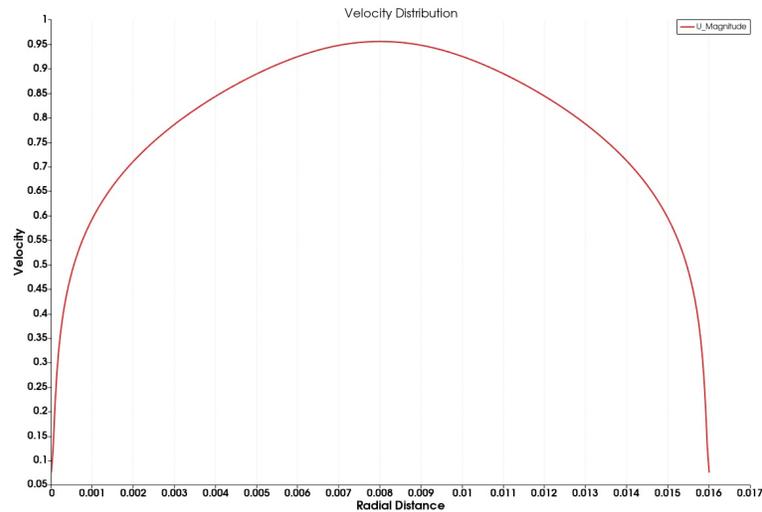
Figure 4.7: Velocity distribution

the flow through the orifice is shown in Figure 4.10. Streamlines for higher and lower Reynolds number cases are shown in Figure 4.11 and 4.12. Vectors were plotted to get a better understanding of the flow as shown in Figure 4.13. Vector plots for higher and lower Reynolds number cases are shown in Figure 4.14 and 4.15 The re-circulation regions are better visualized in the vector plots, and they are circled in red color. Here we can see that the flow converges when it enters the orifice and is accelerated, and at the exit of the orifice the flow expands and diverges, leading to high pressure region. The coefficient of discharge from the CFD results was calculated with pressure predicted by CFD between upstream of orifice and vena-contracta at which the wall pressure is minimum?. The same procedure was carried out for all the other simulations by changing the input values in the U, k and epsilon folder and varying changing the number of cells in the mesh.
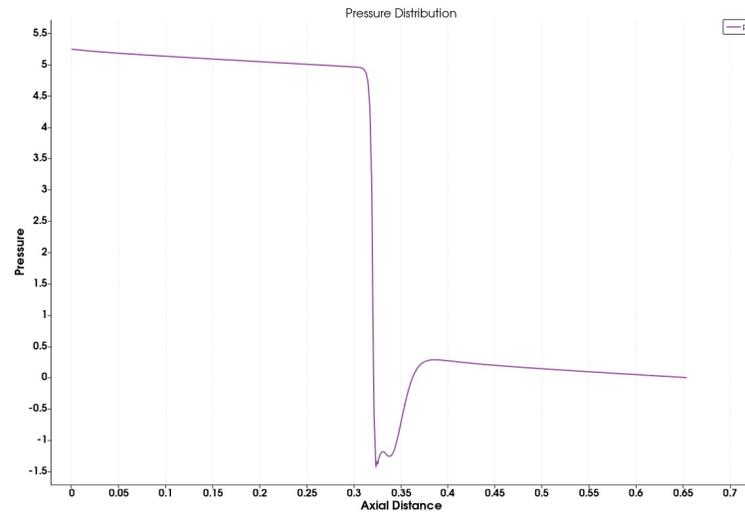
Figure 4.8: Pressure along the axial length
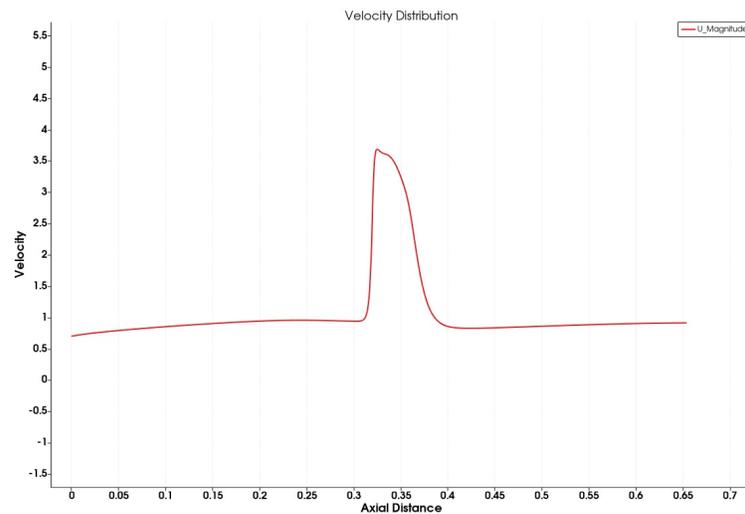


Figure 4.9: Velocity along the axial length

## 4.2  Experimental Results

The experimental data was provided in the manual **?**. The initial and final height of the collecting tank and the manometer's height difference was given. Using the collecting tanks reading, the flow rate was determined and the pressure head was determined using manometer's height difference. With Equation 1.1, the discharge coefficient for experiment data was determined.
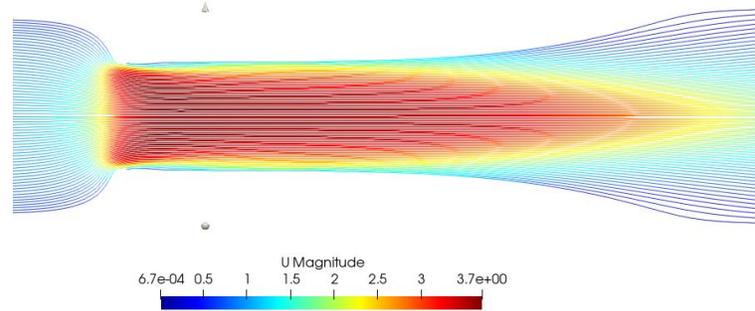
Figure 4.10: Streamlines with velocity scale
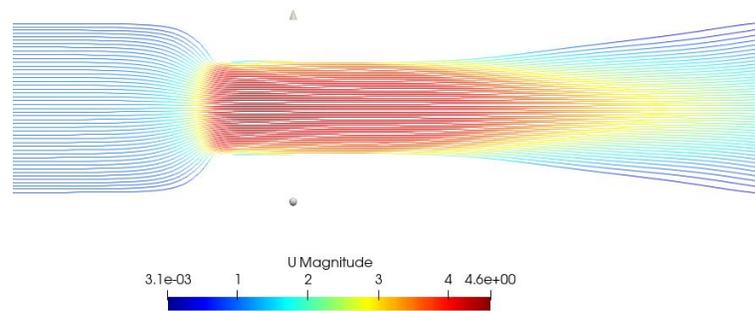


Figure 4.11: Streamlines with velocity scale for higher Reynolds number of 15090
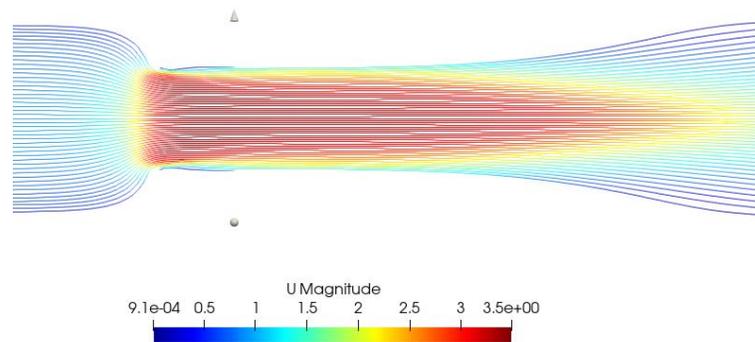


Figure 4.12: Streamlines with velocity scale for lower Reynolds number of 10650

## 4.3   Result comparison

Both the results obtained, CFD and experimental were compared and is summarised
in the Table 4.2 with the input initial conditions for CFD simulations.
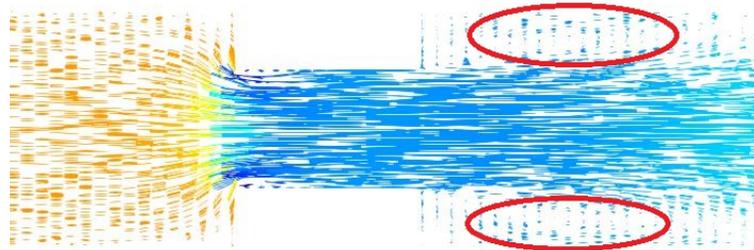
Figure 4.13: Vector Plot
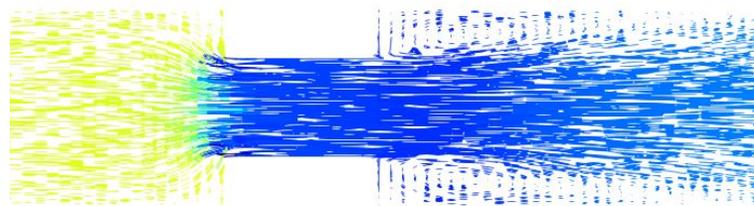


Figure 4.14: Vector Plot for higher Reynolds number of 15090



Figure 4.15: Vector Plot for lower Reynolds number of 10650

From the table we can see that the CFD results obtained is very close to the experimental results. From the table, it can be seen that for Reynolds number greater than 20000, the coefficient of discharge determined was in the range of 0.6-0.66, and for the simulations below this value had the value in the range of 0.7-0.75. To refine the result, two case with low Reynolds number in the range of 6000-8000 was considered and were simulated with low Reynolds number wall boundary

Table 4.1: Low Reynolds number wall boundary conditions

|         | inlet | outlet | wall |
|---------|-------|--------|------|
| epsilon | turbulentMixingLengthDissipationRateInlet | zeroGradient | epsilonWallFunction |
| k | turbulentIntensityKineticEnergyInlet | zeroGradient | kLowReWallFunction |
| nut | calculated | calculated | nutLowReWallFunction |
| p | zeroGradient | fixedValue | zeroGradient |
| U | flowRateInletVelocity | zeroGradient | noSlip |

conditions which is summarised in Table 4.1. In all the files in 0 folder, the axis, front_back_pos and front_back_neg were given the boundary condition of empty, wedge and wedge respectively. The discharge coefficient obtained did not vary much from the previous simulation.

Table 4.2: Experimental and CFD results

| Sl No. | Flow rate($m^3/s$) | Velocity (m/s) | Flow rate($m^3/s$) for $5^0$ wedge | Reynolds number | Turbulent kinetic energy ($m^2/s^2$) | Turbulent dissipation ($m^2/s^3$) | Pressure difference | $C_D$ | $C_D$(exp) |
|---|---|---|---|---|---|---|---|---|---|
| 1 | 0.000141688 | 0.70491478 | 1.96789E-06 | 11278.56 | 1.8484e-3 | 6.386e-3 | 6.6148 | 0.75 | 0.6771 |
| 2 | 0.00015124 | 0.752436107 | 2.10055E-06 | 12038.4 | 2.0724e-3 | 7.58e-3 | 7.55 | 0.749 | 0.6793 |
| 3 | 0.000171306 | 0.852269612 | 2.37925E-06 | 13636.313 | 2.51e-3 | 1.01e-2 | 10.99039 | 0.7038 | 0.7012 |
| 4 | 0.000181862 | 0.904786907 | 2.52586E-06 | 14475.2 | 2.86e-3 | 1.2317e-2 | 10.99742 | 0.746 | 0.6981 |
| 5 | 0.00020152 | 1.00258698 | 2.79889E-06 | 16040 | 3.416e-3 | 1.6e-2 | 13.23151 | 0.7545 | 0.7378 |
| 6 | 0.000204571 | 1.017767353 | 2.84127E-06 | 16283.2 | 3.52e-3 | 1.67e-2 | 14.10243 | 0.7417 | 0.6318 |
| 7 | 0.000189579 | 0.943181434 | 2.63305E-06 | 15089.6 | 3.07e-3 | 1.36e-2 | 13.3768 | 0.7057 | 0.6637 |
| 8 | 0.000231358 | 1.151037266 | 3.21331E-06 | 18416 | 4.352e-3 | 2.307e-2 | 17.67421 | 0.7495 | 0.8004 |
| 9 | 0.000256527 | 1.27625471 | 3.56288E-06 | 20419.2 | 5.21e-3 | 3.025e-2 | 27.36814 | 0.6678 | 0.8049 |
| 10 | 0.00027642 | 1.375224868 | 3.83917E-06 | 22003.2 | 5.950e-3 | 3.6885e-2 | 37.7191 | 0.6130 | 0.82 |
| 11 | 8.38141E-05 | 0.416985476 | 1.16408E-06 | 6670.4 | 7.3786e-4 | 1.61e-3 | 2.34602 | 0.7453 | 0.765 |
| 12 | 9.73175E-05 | 0.484166469 | 1.35163E-06 | 7745.6 | 9.5786e-4 | 2.38e-3 | 3.147181 | 0.7471 | 0.6115 |
| 13 | 0.000133894 | 0.666138623 | 1.85964E-06 | 10657.6 | 1.670e-3 | 5.486e-3 | 5.94225 | 0.7481 | 0.801 |
| 14 | 8.56285E-05 | 0.426012396 | 1.18928E-06 | 6816 | 7.646e-4 | 1.699e-3 | 2.434624 | 0.7474 | 0.586 |
| 15 | 0.000111473 | 0.554590683 | 1.54823E-06 | 8872 | 1.213e-3 | 3.3979e-3 | 4.132407 | 0.7469 | 0.6557 |

# Chapter 5

# Conclusion

In this project, simulation of turbulent flow through an orifice meter was done using $\kappa$ -$\epsilon$ RANS turbulence model.The coefficient of discharge was determined for 15 different cases and Reynolds number in the range of 6000-20000. The obtained discharge coefficient was compared with experimentally obtained values. Velocity and pressure contours and streamlines were visualised through which various distinctive flow behaviours were studied.